Desalination and Water Treatment
www.deswater.com
doi: 10.5004/dwt.2021.27625

240 (2021) 115–123
November

The inhibition of precipitation of calcium carbonate scale by *Eucalyptus globulus* leaves extract as green inhibitor

Ilham Karmal[a,b,*], Mohamed El Housse[a], Abdallah Hadfi[a], Jamila El Gaayda[b], Abdallah Oulmekki[c], Jamal Eddine Hazm[c], Said Ben-Aazza[a], M'barek Belattar[a], Said Mohareb[a], Naima Hafid[a], Rachid Ait Akbour[b], Mohamed Hamdani[b], Ali Driouiche[a]

[a]*Team "Materials and Water Physico-Chemistry", Laboratory of Process Engineering, Faculty of Sciences, IBN ZOHR University, P.O. Box: 8106, Agadir, Morocco, emails: ilham.karmal@edu.uiz.ac.ma (I. Karmal), elhousse.mohamed@gmail.com (M. El Housse), hadfiabd@yahoo.fr (A. Hadfi), bn.said@yahoo.fr (S. Ben-Aazza), belattar100@hotmail.fr (M. Belattar), moharebsaid@gmail.com (S. Mohareb), hafidnaima@yahoo.fr (N. Hafid), driouiche@yahoo.fr (A. Driouiche)*
[b]*Team Electrochemistry and Environment, Faculty of Sciences, IBN ZOHR University, P.O. Box: 8106, Agadir, Morroco, emails: elgaayda.jamila@gmail.com (J. El Gaayda), ak04rach@hotmail.fr (R.A. Akbour), hamdani.mohamed@gmail.com (M. Hamdani)*
[c]*Laboratory of Condensed Matter Chemistry, Faculty of Science and Technology, Sidi Mohamed Ben Abdellah University, B.P. 2202, Fes, Morroco, emails: abdallah.oulmekki@usmba.ac.ma (A. Oulmekki), jamaleddine.hazm@usmba.ac.ma (J. Eddine Hazm)*

Received 28 May 2021; Accepted 7 July 2021

ABSTRACT

In this study, we investigate the effect of aqueous extract of *Eucalyptus globulus* leaves (EGL) as a new green inhibitor on the precipitation of calcium carbonate ($CaCO_3$) by using the rapid controlled precipitation method in synthetic solution. The EGL inhibitory characteristics were studied using several parameters including pH, calcium, and bicarbonate ions concentrations. The obtained results revealed that the inhibitory capacity of the EGL extract is proportional to its concentration. The total inhibition of $CaCO_3$ precipitation was achieved after adding a low concentration of 75 mg/L. Moreover, the precipitation threshold of $CaCO_3$ occurs at a higher germination time and lower supersaturation coefficient with a dissolved CO_2 outgassing rate. The mechanism of inhibition scaling by EGL was proposed. Therefore, *E. globulus* leaves could be taken as a novel scale inhibitor on reverse osmosis membrane.

Keywords: Green inhibitor; Calcium carbonate; Inhibition; Scale inhibitor; Reverse osmosis

1. Introduction

In the last decades, in the areas of the world in which people suffer from water scarcity, water reclamation strategies are becoming increasingly relevant [1–3]. Owing to the excellent and reliable performance of different rejects (ions, microorganisms, and organic pollutants), reverse osmosis (RO) technology has proved to be an effective treatment strategy. However, in addition to providing highly cleaned water for potable reuse [4,5], fouling is a common problem with RO membrane systems.

Scaling is the term for inorganic fouling. It is defined as the formation of deposits due to the precipitation of poorly soluble salts when a surface comes into contact with water [6]. The formation of this deposit in water systems such as industrial systems, domestic systems, wastewater reuse systems, groundwater exploitation systems, seawater, and brackish water desalination systems has been widely known as a major problem [7–10]. In reverse

* Corresponding author.

Presented at the Second International Symposium on Nanomaterials and Membrane Science for Water, Energy and Environment (SNMS-2021), June 1–2, 2022, Tangier, Morocco

osmosis membranes, the deposits could alter their performance associated with permeate flow and salt rejection as well as decrease their life span which leads to economic losses [11,12]. This condition usually arises whenever the membrane surface gets excessive salt concentration beyond the solubility limitations.

One of the most prevalent scale deposits is calcium carbonate ($CaCO_3$). As known, the $CaCO_3$ exists in different forms such as amorphous calcium carbonate, calcite, aragonite, and vaterite [13–15]. Nevertheless, the calcium carbonate scale is easily deposited after its solubility limit has exceeded which is due to its low solubility in water or the systems are saturated with scaling ions. Also, the precipitates of calcium carbonate are the result of external modifications of specific factors [16]. These precipitates cause many problems such as increased energy consumption, restricted fluid flow, and equipment damage, and then leave negative aspects in membrane processes. On the other hand, the calcium carbonate crystals tend to form hard deposits on the exchange surfaces of brackish water treatment reverse osmosis, which leads to fouling and failure of reverse osmosis modules. For these reasons, many efforts have been made to delay or inhibit $CaCO_3$ formation by using several methods (i.e., the physical methods and the chemical methods) [17,18]. In most cases, the only way to remove precipitated calcium carbonate is by scraping or cleaning which is impractical and expensive. Therefore, inhibitors have been used in various applications thanks to their cost-effectiveness and high performance [19–22]. The use of these inhibitors in the RO feed stream instead of acid injection helps to reduce the possibility of scaling [23–25]. Because they can interfere with deposit formation during crystallization processes and scale nucleation in a variety of ways, including crystal modification, dispersion, threshold inhibition, crystal, and chelation [26–28]. The experimental determination of antiscalant effectiveness has been generally studied by several methods, namely: the critical pH method, LCGE method, rapid controlled precipitation method, chronoelectrogravimetry, and electrochemical impedance technique [29]. Scale inhibitors largely retard the rate of crystal growth in an aqueous solution and the behavior of the crystals can be modified. However, chemical inhibitors are no longer recommended for the treatment of drinking water for human consumption. As a result, the "green scaling inhibitor" has become a popular research topic in recent years. Green inhibitors have no harmful effects on the human body. Plant extracts are becoming increasingly popular thanks to their availability, cheapness, renewability, and great performance [30,31].

In this study, *Eucalyptus globulus* leaves (EGL) were selected as a green antiscalant to protect the RO system. *E. globulus* is an evergreen tree native to Australia and cultivated in the Mediterranean and subtropical areas [32], indeed, it is very abundant in Morocco especially in the region of Souss Massa. Its leaves have been used as raw material for food, nutritional, and pharmaceutical supplements thanks to being bioactive, antioxidant, and neuroprotective properties [33,34]. Moreover, they contain main chemical compounds such as terpenoids and polyphenols, flavonoids, and tannins [35]. Thus, *E. globulus* leaves can be used as an alternative and cheap way to reduce the growth of scale deposits. The objective of this research was to examine the efficiency of inhibiting or preventing the formation of $CaCO_3$ on the RO membrane during operation, by the extract of EGL. This inhibitor was prepared by infusion. A series of inhibition experiments by green inhibitor effect, including monitoring of a set of measurements of pH, calcium hardness (*T*Ca), complete alkalimetric titer (TAC), a supersaturation coefficient (β), partial pressure of CO_2 (P_{CO_2}), and then carried out for the study of scaling in order to describe the kinetics of precipitation. Finally, the mechanism of inhibition scaling by EGL was proposed.

2. Materials and methods

2.1. Reagents

Sulfuric acid (H_2SO_4), calcium carbonate ($CaCO_3$), ethylenediaminetetraacetic acid (EDTA), ammonia (NH_3), and ammonium chloride (NH_4Cl) were obtained from Sigma-Aldrich. Methyl orange (indicator), hydrochloric acid (HCl), and Eriochrome Black T (indicator) were purchased from Loba Chemie. All of these reagents were reagent grade and directly used without further purification.

2.2. Synthetic solution

The synthetic solution is pure calco-carbonic water. It was prepared using a high-quality analytical product ($CaCO_3$) by dissolving 0.4 g L^{-1} of calcium carbonate in bi-distilled water, to simulate the impact of green inhibitor presence over the germination time of $CaCO_3$. Its preparation was done under the bubbling of carbonic (CO_2) for complete solubilization of $CaCO_3$ during 30 min under magnetic stirring, following the reaction given below:

$$CaCO_3 + H_2O \leftrightarrow Ca^{2+} + 2HCO_3^- \quad (1)$$

2.3. Preparation of E. globulus extract

E. globulus leaves (EGL) were harvested during February in the Souss Massa region (Agadir, Morocco). It was oven-dried at a temperature of 40°C for 24 h. Also, they were pulverized with a closed electric mill to obtain a fine powder. The aqueous extract solution was obtained by adding 100 mL of distilled water to 5 g of plant and let it boil for 1 h. After that, it was filtered through a filter paper of 0.45 μm pores. The pH of the plant extract was initially slightly acidic (pH 5.8). The extract was obtained after drying the aqueous solution and then stored until its use. For inhibition tests, appropriate amounts of this extraction were prepared and added to the calco-carbonic solution.

2.4. Fourier transform infrared spectrum

A Fourier transform infrared spectroscopy (FTIR) Thermo-Nicolet spectrometer (AVATAR 320 AEK0200713) was used for characterizing the EGL extract. The spectra were recorded in the wavenumber range of 400 to 4,000 cm^{-1}. The FTIR was executed to identify the sample functional group of EGL extract.

2.5. LCGE controlled degassing method

Roques and his partners created this method [36,37], which is known as the Laboratory of Chemistry and Environmental Engineering (LCGE). It allows for the separation of the many kinetic processes in order to isolate the one that is the most typically kinetically limiting, namely the matter transfer at the liquid/solid interface. Water degassing (displacement of the calco-carbonic equilibrium in the direction of calcium carbonate formation) to be examined by a working gas, most commonly via atmospheric air, is a major of cause calcium carbonate precipitation. The latter is the main engine of a system evolution leading to scaling as shown by the following reaction [38]:

$$Ca^{2+} + 2HCO_3^- \leftrightarrow CaCO_3 + CO_2 + H_2O \quad (2)$$

The experimental cell contains 500 mL of the solution to be studied. It was then kept in a thermostatic bath to keep the temperature at 30°C (Fig. 1). The cell is equipped with a gas inlet (atmospheric air) at the bottom of a perforated bottom, which ensures its uniform dispersion in the whole solution. The gas flow rate is set at 8 L/min for all experiments. During the test, the pH, calcium titer, and full alkalimetric titer of the solution were measured continuously every 2 min by a pH meter (Hanna HI 5221). The concentration of calcium and bicarbonate ions was determined by the complexometric EDTA titration and acid titration, respectively. The CO_2 partial pressure and supersaturation can be calculated using the evolution of pH and calcium titer over time. These parameters allow a complete description of the precipitation kinetics.

3. Results and discussion

3.1. Characterization of scale deposits on the reverse osmosis membranes

Scale deposits on reverse osmosis membranes were structurally and morphologically characterized in detail and the results are presented in our previous literature [39].

3.2. Functional group characterization of EGL extract

An FTIR analysis was used to identify some functional groups found in the *E. globulus* leaves powder. As seen in Fig. 2, a broad band at 3,281 cm^{-1} is attributed to the stretching of the hydroxyl group [40]. The appearance of the O–H band's vibration at 3,200–3,431 cm^{-1} is an indication of the presence of phenolic [41]. The band located at 2,928 cm^{-1} is assigned to the C–H stretching vibration of aliphatic hydrocarbons absorption, and a band at 2,864 cm^{-1} corresponds to the C–H stretching of aldehydes. In regards to phenolic compounds attributed bands, the FTIR spectrum of EGL shows bands at 1,631 cm^{-1} indicates the stretching vibration of the C=C, 1,341 cm^{-1} due to the C–N stretching vibration for aromatic amines, and 1,040 cm^{-1} for the C–N stretching vibration of aliphatic amines, respectively [42]. These results are similar to those obtained by Saleem et al. [35] and Wang et al. [43].

3.3. Evaluation of the scale inhibition performance by LCGE tests

3.3.1. Effect of green inhibitor (EGL) on pH

The pH vs. time curves is shown in Fig. 3. It is indicated that when the concentration of EGL was lower than

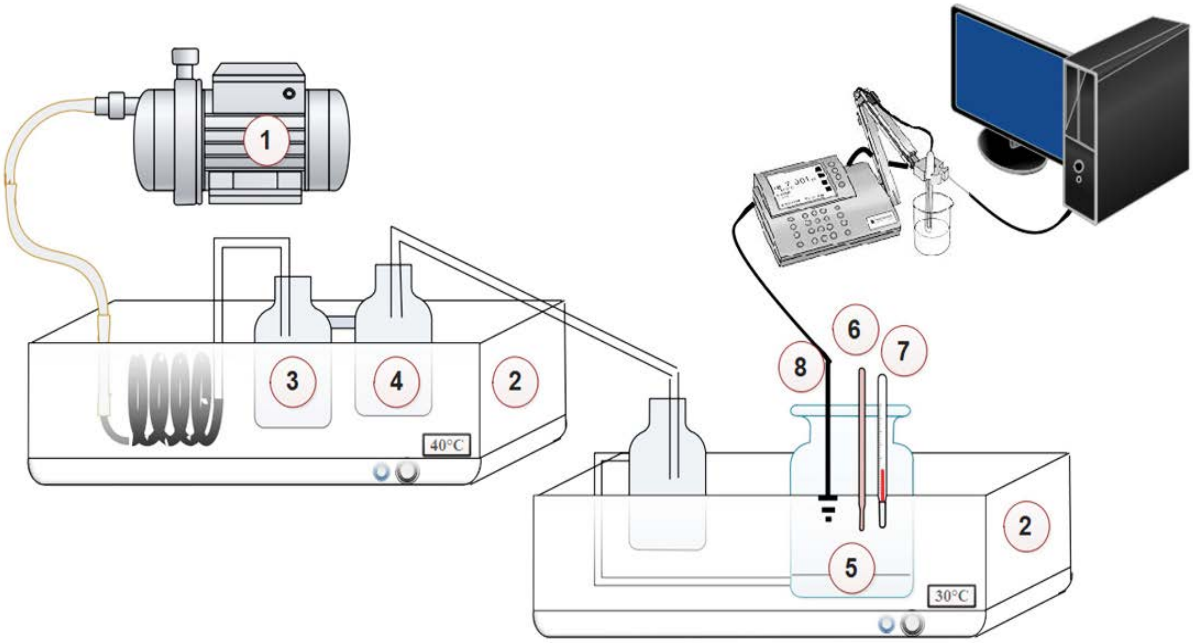

Fig. 1. Experimental setup of the LCGE method. 1: Stripping gas; 2: Thermostatic baths; 3: Humidifier; 4: Humidity traps; 5: Work cell; 6: Simple taken for dosage of [Ca^{2+}] and TAC; 7: Temperature sensor; 8: pH meter.

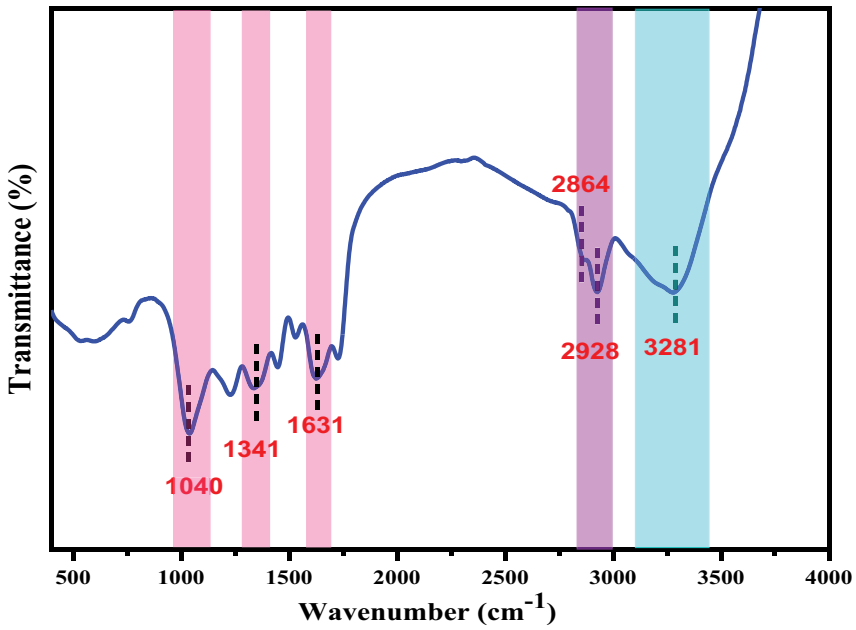

Fig. 2. IR spectrum of EGL powder.

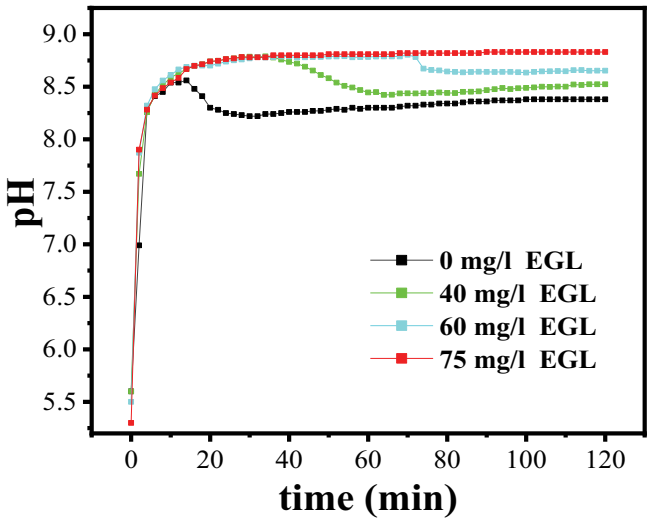

Fig. 3. pH – time curves during the precipitation of $CaCO_3$ in different concentrations.

75 mg/L, the inhibition of scaling in the calco-carbonic solution was hardly affected, and when it was higher than 75 mg/L, the effectiveness of total inhibition was observed during the 120 min of the experience.

At the germination points, the pH of untreated water was found to be 8.56 and then dropped quickly. The pH-time curves extended linearly to the right when the inhibitor was added, and no precipitate emerged during the experience. The germination pH (pH_g) values increase due to hydrolysis of CO_3^{2-} to OH^-, and the pH drops were less abrupt when the inhibitor was added. This reflects the start of $CaCO_3$ precipitation and then becomes stable. The two responses of gas transport at the liquid/gas interface and chemical reaction in the liquid phase are reflected in this change in pH. The precipitation reaction of calcium carbonate is pH-depending [44], as shown in Eq. (3):

$$Ca^{2+} + HCO_3^- + H_2O \leftrightarrow CaCO_3 + H_3O^+ \quad (3)$$

According to Table 1, which summarizes the main experimental results, the germination time without inhibitor was 14 min. The germination time was only 34 min and the minor effects on scaling inhibition were found even after the introduction of 40 mg/L EGL. The T_g began to drop 70 min later in water treated with 60 mg/L EGL than in untreated water. Thus, with the addition of EGL extract, the pH_g values increased, indicating a low carbonate consumption, and then a decrease in $CaCO_3$ precipitation. The germination time became longer with the addition of EGL, as shown in Fig. 3. The pH_g increases with the EGL concentration, which can be due to the presence of more polyphenols existing in EGL extract will react to Ca^{2+} ions to inhibit the formation of $CaCO_3$ nuclei. Therefore, shows a double effect according to this comparison of pH-time curves. This variation of pH reflects both responses of chemical reaction in a liquid phase and gas transfer at the gas/liquid interface. As a result, it approves that the property of EGL has a direct effect on calcium carbonate precipitation.

3.3.2. *Effect of green inhibitor (EGL) on TCa and β_{cal}*

As shown in Fig. 4a, the calcium ions concentration does not vary at the beginning of the experiment. However, the volumetric measurement is done after every 2 min. The obtained results of experiments show the formation of the first colloidal nuclei of $CaCO_3$, which due to the fact that the decrease of calcium ions indicates the beginning of precipitation. In this stage, the solution became slower (Fig. 4a)

Table 1
Values of pH_g and germination time tested by pH measurement testing in different concentrations

Inhibitor (mg/L)	0	40	60	75
pH_g	8.56	8.78	8.80	8.83
Germination time (min)	14	34	70	–

with the increase of EGL concentration reflects the prevention of Ca^{2+} binding to CO_3^{2-} in the solution decreased accordingly. It then gradually decreases as equilibrium conditions are approached. It should be noted that the germination time calculated using the *T*Ca = *f*(*t*) curve is identical to that calculated using the pH = *f*(*t*) curve.

Kezia describes the $CaCO_3$ crystallization as a multistep process that includes crystal development, recrystallization, germination, and agglomeration [45]. The degree of supersaturation is the most important factor in germination and development [46].

The supersaturation coefficient (β) could be computed via the ratio of dissolved $CaCO_3$'s ionic activity product to its solubility product (K_s), which is mentioned in Eq. (4) [47]:

$$\beta = \frac{\left(Ca^{2+}\right)\left(CO_3^{2-}\right)}{K_s} = \frac{\gamma_{Ca^{2+}}\left[Ca^{2+}\right]\gamma_{CO_3^{2-}}\left[CO_3^{2-}\right]}{K_s} \quad (4)$$

where $[Ca^{2+}]$ and $[CO_3^{2-}]$ are calcium and carbonate ions concentrations, respectively, while that of $\gamma_{Ca^{2+}}$ and $\gamma_{CO_3^{2-}}$ are activity coefficients of $[Ca^{2+}]$ and $[CO_3^{2-}]$, respectively. The divergence of the system from its steady-state is represented by these supersaturation values at the germination point [48]. Three primary regions can be seen in Fig. 4b. The first is a quick increase in β, where the β inclined to highest called β germination (β_g), which is connected with a lack of Ca^{2+} precipitation before germination time. A rapid decrease in the supersaturation coefficient characterizes the second region coincides with the onset of homogeneous $CaCO_3$ precipitation. The supersaturation coefficient-loaded the third phase corresponds to precipitation end leads to a constant value.

Table 2 shows that the increase in findings as the EGL concentration increased, indicating that an exceptionally high EGL concentration could inhibit the $CaCO_3$ precipitation.

3.3.3. Influence of green inhibitor (EGL) on TAC and P_{CO_2}

Fig. 5a and b shows the evolution of TAC and P_{CO_2} as a function of time. The partial pressure (P_{CO_2}) can be calculated as follows:

$$P_{CO_2} = \frac{D \cdot T\text{Ca} \cdot 10^{K_1 - \text{pH}}}{\frac{2.10^{\text{pH}-K_2}}{f_{CO_3^{2-}}} + \frac{1}{f_{HCO_3^-}}} \quad (5)$$

where K_1 and K_2 are the dissociation constants of carbonic acid; f_a is the activity coefficient of the species *a*; and *D* is Henry's law constant (mol^{-1} L atm).

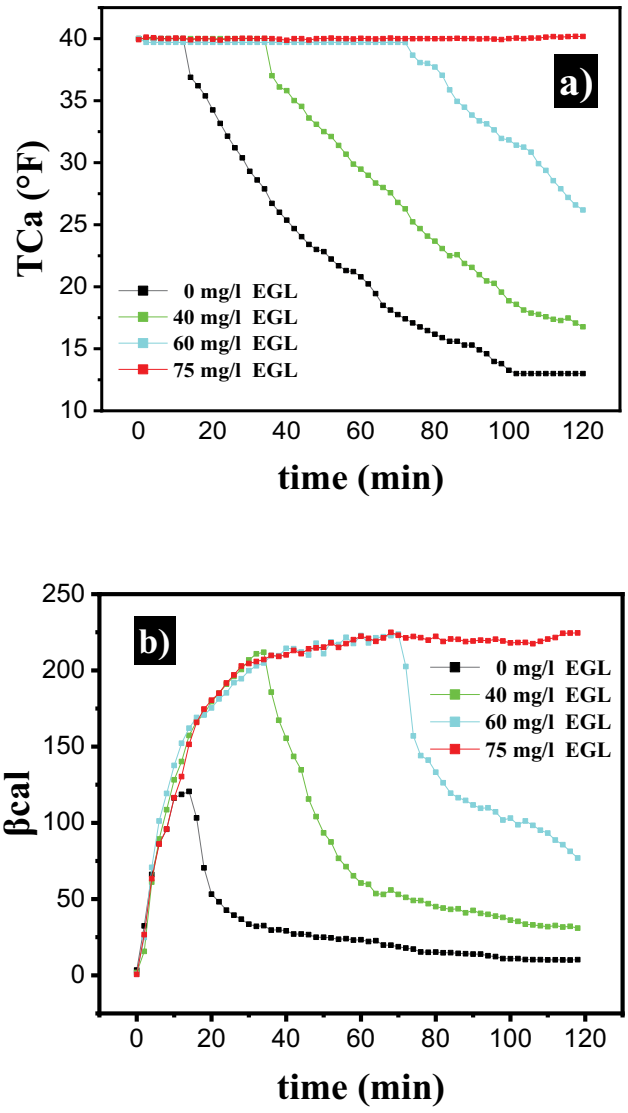

Fig. 4. $[Ca^{2+}]$ – time curves (a) and β_{cal}– time curves (b) during the precipitation of $CaCO_3$ in different concentrations.

Table 2
Values of β_g and germination time tested by β_{cal} measurement testing in different concentrations

Inhibitor (mg/L)	0	40	60	75
β_g	120.62	211.87	223.77	224.57
Germination time (min)	14	34	70	–

The findings demonstrated that there was a stability period at the start of the experiment. Throughout this stage, the TAC values stabilize associated with a decrease in P_{CO_2}. Consequently, no possibility of germination was observed. It can be observed that before the addition of EGL, the precipitation started. However, for EGL values up to 60 mg/L, there is a decrease in TAC after 70 min, accompanied by an increase in P_{CO_2} indicated the germination of $CaCO_3$, following this reaction:

$$Ca^{2+} + HCO_3^- \leftrightarrow CaCO_3 + H^+ \quad (6)$$

At 75 mg/L of EGL (efficiency concentration), the inhibition is complete and no extra calcium carbonate precipitation occurs.

3.4. Kinetic study

For the kinetic exploitation of the $CaCO_3$ precipitation results, we used a calculation program. This program allows the systematic exploitation of the experimental results of the two models diffusional and Reddy. The diffusional model is the first-order model which was used for the exploitation of the results of precipitation of $CaCO_3$ in the most stable forms (calcite) [39]. Then the Reddy model is the second-order model which was used in different operating conditions. A linear regression program establishes the correlation line in each example, providing the correlation coefficient (R^2) and the rate constant for the comparability of fits made [49].

Expressing the Ca^{2+} concentrations in French hydrotimetric degree, we will have:

(Diffusional Model) first-order

$$\ln\frac{TCa - TCa_{eq}}{TCa_0 - TCa_{eq}} = K_T \cdot t \quad (7)$$

(Reddy Model) second-order

$$\frac{1}{TCa - TCa_{eq}} - \frac{1}{TCa_0 - TCa_{eq}} = K_T \cdot t \quad (8)$$

where K_T is the global speed constant; TCa_0 is the initial Ca^{2+} concentration; and TCa_{eq} is the concentration at thermodynamic equilibrium.

According to the analysis of the curves presented in Figs. 3, 4 and 5 and the kinetic modeling, the different values of the rate constants, with respect to calcite, are represented in Table 3. For inhibitor doses of 0–60 mg/L, the pH_g tends to increase by 8.83–9.23 at the start of precipitation. The decrease in pH is more obvious in the test in the absence of an inhibitor, but it gets less noticeable as the concentration increases. After the introduction of EGL, there was an increase in the degree of supersaturation. Then, as compared to the control test, the germination time is longer. As a result, the precipitation kinetics for the assay in the presence and absence of inhibitor *E. globulus* leaves follow a diffusion model.

3.5. Mechanism of inhibition of $CaCO_3$

The inhibition mechanism of EGL extract is illustrated in Fig. 6. This extract contains different antioxidants, mainly contained in a large amount of polyphenols and flavonoids

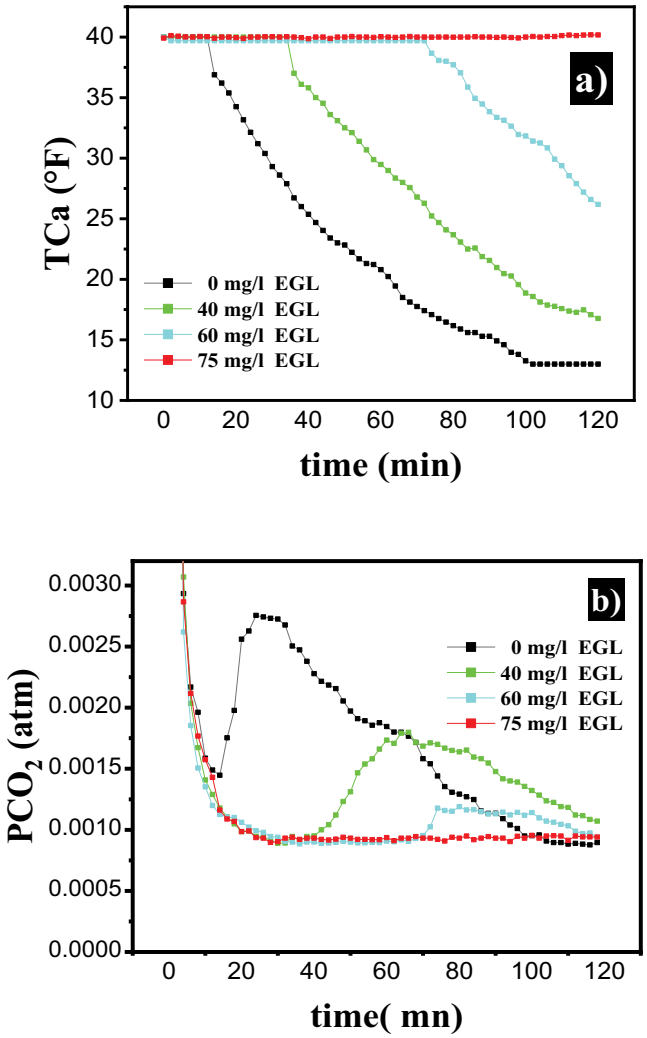

Fig. 5. TAC – time curves (a) and P_{CO_2} – time curves (b) during the precipitation of $CaCO_3$ in different concentrations.

Table 3
Variation of T_g, pH_g, β_g, and kinetic constants (K_D: diffusional and K_R: Reddy) as a function of the increasing quantities of inhibitor

P_{CO_2} gaz = 3 × 10⁻⁴ atm	Concentration (mg/L)	T_g (min)	pH_g	β_g	Diffusional calcite		Reddy calcite	
					K_D (mn⁻¹)	R^2	K_R (F⁻¹ mn⁻¹)	R^2
Without inhibitor	0	14	8.56	120.62	1.41 × 10⁻²	0.991	8.32 × 10⁻⁴	0.978
	40	34	8.78	211.87	1.22 × 10⁻²	0.990	5.49 × 10⁻⁴	0.957
With inhibitor	60	70	8.80	223.77	9.74 × 10⁻³	0.966	3.47 × 10⁻⁴	0.957
	75	–	8.83	224.57	–	–	–	–

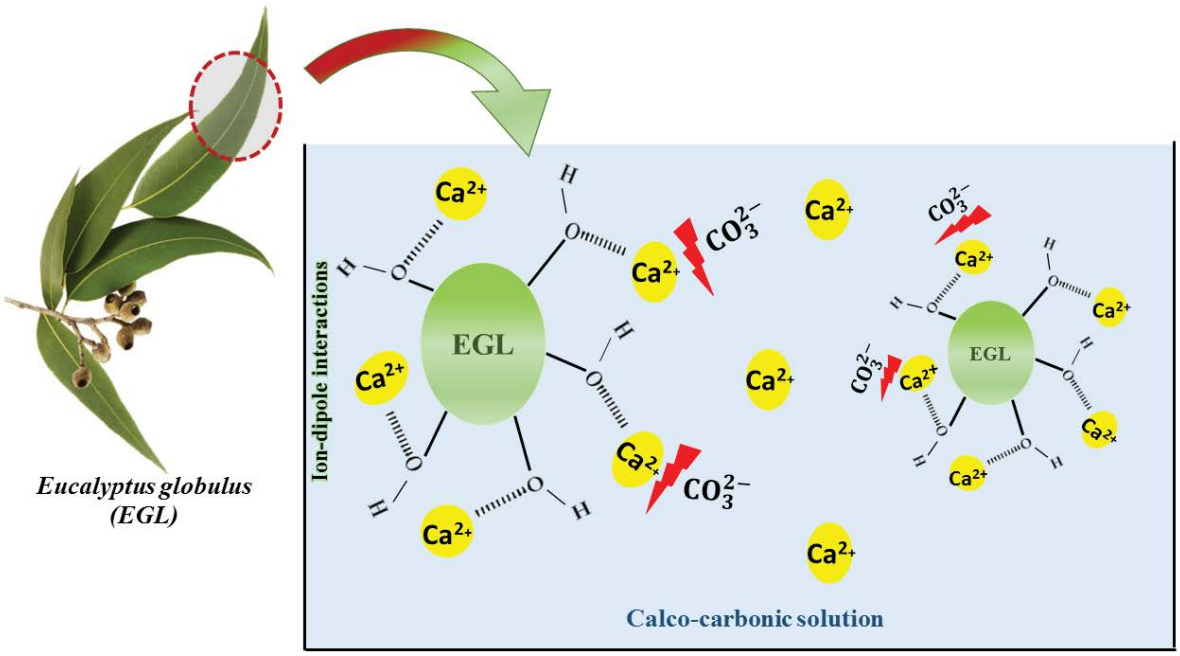

Fig. 6. Mechanism of scaling inhibition of $CaCO_3$ using EGL.

[34]. Agarwal et al. [50] show that the polyphenols and flavonoids are responsible for the inhibition of $CaCO_3$ formation by reacting with Ca^{2+} ions present in water [50]. On this subject, polyphenols possess –OH functional groups that interact with the Ca^{2+} ion by ion-dipole interaction. Thus, OH groups prevent calcium ions from reacting with carbonate ions, and then this interaction causes the reversible reaction of $CaCO_3$ [Eq. (9)], and as a result, the formation of $CaCO_3$ will be decreased. The obtained results show that EGL can be used as a greater inhibitor of $CaCO_3$ in desalination water.

$$Ca^{2+} + CO_3^{2-} \rightleftarrows CaCO_3 \quad (9)$$

4. Conclusion

In this work, *E. globulus* leaves extract (EGL) was tested as an inhibitor to control scaling in controlled laboratory experiments. Inhibition tests confirmed that EGL has a strong ability to effectively inhibit $CaCO_3$ formation and growth. LCGE tests were performed using several key parameters that could affect the inhibition performance of $CaCO_3$ formation. The results revealed that when the concentrations of EGL were below 75 mg/L, practically a small inhibition effect on $CaCO_3$ scaling could be observed. However, when the doses were increased to 75 mg/L, full inhibition could be achieved during the 120 min of the experience with the percentage of inhibitor efficiency 100%. Nevertheless, its inhibition power is pH dependent. The pH_g rises with the inhibitor concentration from 8.65 for 0 mg/L to 8.83 for 75 mg/L. Thus, this work not only provided information on the use of the EGL extract to inhibit $CaCO_3$ formation, but also argued that the use of the EGL extract to control scaling can serve as an environment-friendly scale inhibitor; and then can be considered as a green product for treating drinking water.

Symbols

(Ca^{2+})	—	Activity of the ion Ca^{2+}
$[Ca^{2+}]$	—	Ca^{2+} concentration
(CO_3^{2-})	—	Activity of the ion CO_3^{2-}
$[CO_3^{2-}]$	—	CO_3^{2-} concentration
D	—	Henry's law constant, mol^{-1} L atm
f_a	—	Activity coefficient of the species a
K_s	—	Solubility product
K_1 and K_2	—	Dissociation constants of carbonic acid
K_D	—	Calcite diffusional constant
K_R	—	Reddy's constant calcite
K_T	—	Global speed constant
P_{CO_2}	—	Partial pressure
pH	—	potential of hydrogen
t	—	Induction time
TCa	—	Ca^{2+} concentration
$T\text{Ca}_0$	—	Initial Ca^{2+} concentration
$T\text{Ca}_{eq}$	—	Ca^{2+} Concentration at thermodynamic equilibrium

Greek letters

β	—	Supersaturation coefficient
β_{cal}	—	Coefficient of supersaturation with respect to calcite
$\gamma_{Ca^{2+}}$	—	Activity coefficients of $[Ca^{2+}]$
$\gamma_{CO_3^{2-}}$	—	Activity coefficients of $[CO_3^{2-}]$

References

[1] Y. Naciri, A. Hsini, A. Bouziani, R. Djellabi, Z. Ajmal, M. Laabd, J.A. Navío, A. Mills, C.L. Bianchi, H. Li, B. Bakiz, A. Albourine, Photocatalytic oxidation of pollutants in gas-phase via Ag_3PO_4-based semiconductor photocatalysts: recent progress,

new trends, and future perspectives, Crit. Rev. Env. Sci. Technol., (2021) 1–44, doi: 10.1080/10643389.2021.1877977.
[2] A. Hsini, Y. Naciri, M. Laabd, M. El Ouardi, Z. Ajmal, R. Lakhmiri, R. Boukherroub, A. Albourine, Synthesis and characterization of arginine-doped polyaniline/walnut shell hybrid composite with superior clean-up ability for chromium(VI) from aqueous media: equilibrium, reusability and process optimization, J. Mol. Liq., 316 (2020) 113832, doi: 10.1016/j.molliq.2020.113832.
[3] H. Barebita, Y. Naciri, S. Ferraa, A. Nimour, T. Guedira, Investigation of structural and photocatalytic behavior of $Bi_{13}B_{1-2x}V_xP_xO_{20.95+2x}$ ($0 \le x \le 0.5$), Solid State Sci., 108 (2020) 106389, doi: 10.1016/j.solidstatesciences.2020.106389.
[4] H.L. Leverenz, G. Tchobanoglous, T. Asano, Direct potable reuse: a future imperative, J. Water Reuse Desalin., 1 (2011) 2–10.
[5] D. Gerrity, B. Pecson, R. Shane Trussell, R. Rhodes Trussell, Potable reuse treatment trains throughout the world, J. Water Supply Res. Technol. - AQUA., 62 (2013) 321–338.
[6] N. Penña, S. Gallego, F. del Vigo, S.P. Chesters, Evaluating impact of fouling on reverse osmosis membranes performance, Desal. Water Treat., 51 (2013) 958–968.
[7] A. Hadfi, H. Eddaoudi, M. El Hadek, A. Ghorbel, A. Driouiche, Characterization of scale-forming power of irrigation water the agricultural region of large Agadir Caracterisation du pouvoir entartrant des eaux d'irrigation de la region agricole du grand Agadir, Phys. Chem. News, 57 (2011) 44–50.
[8] S. Ben-aazza, A. Hadfi, S. Mohareb, I. Karmal, M. Belattar, N. Hafid, A. Driouiche, Geochemical characterization and thermodynamic study of water scaling phenomenon at Tiznit region in Southern Morocco, Groundwater Sustainable Dev., 11 (2020) 100379, doi: 10.1016/j.gsd.2020.100379.
[9] S. Mohareb, I. Karmal, A. Hadfi, S. Ben-aazza, M. Belattar, N. Hafid, M. El Housse, A. Driouiche, Investigation of pipes and sprinklers scaling at the golf course turf irrigated by treated wastewater of Mzar plant in Agadir-Morocco, Mediterr. J. Chem., 9 (2020) 440–446.
[10] N. Hafid, M. Belaatar, S. Ben-Aazza, A. Hadfi, M. Ezahri, A. Driouiche, Characterization of scale formed in drinking water and hot water pipes in the Taliouine downtown—Morocco, Am. J. Anal. Chem., 6 (2015) 677, doi: 10.4236/ajac.2015.68065.
[11] S. Shirazi, C.J. Lin, D. Chen, Inorganic fouling of pressure-driven membrane processes – a critical review, Desalination, 250 (2010) 236–248.
[12] A. Sweity, Z. Ronen, M. Herzberg, Induced organic fouling with antiscalants in seawater desalination, Desalination, 352 (2014) 158–165.
[13] H. Wang, V. Alfredsson, J. Tropsch, R. Ettl, T. Nylander, Formation of $CaCO_3$ deposits on hard surfaces – effect of bulk solution conditions and surface properties, ACS Appl. Mater. Interfaces., 5 (2013) 4035–4045.
[14] W. Mejri, A. Korchef, M. Tlili, M. Ben Amor, Effects of temperature on precipitation kinetics and microstructure of calcium carbonate in the presence of magnesium and sulphate ions, Desal. Water Treat., 52 (2014) 4863–4870.
[15] Y. Usmany, W.A. Putranto, A.P. Bayuseno, S. Muryanto, Crystallization of calcium carbonate ($CaCO_3$) in a flowing system: influence of Cu^{2+} additives on induction time and crystalline phase transformation, AIP Conf. Proc., 1725 (2016) 020093, doi: 10.1063/1.4945547.
[16] B. Bouargane, M.G. Biyoune, A. Mabrouk, A. Bachar, B. Bakiz, H. Ait Ahsaine, S. Mançour Billah, A. Atbir, Experimental investigation of the effects of synthesis parameters on the precipitation of calcium carbonate and portlandite from Moroccan phosphogypsum and pure gypsum using carbonation route, Waste Biomass Valorization, 11 (2020) 6953–6965.
[17] I. Atamanenko, A. Kryvoruchko, L. Yurlova, E. Tsapiuk, Study of the $CaSO_4$ deposits in the presence of scale inhibitors, Desalination, 147 (2002) 257–262.
[18] W.J. Liu, F. Hui, J. Lédion, X.W. Wu, Inhibition of scaling of water by the electrostatic treatment, Water Resour. Manage., 23 (2009) 1291–1300.
[19] M. El Housse, A. Hadfi, I. Karmal, S. Ben-aaza, M. Belattar, M. Errami, S. Mohareb, A. Driouiche, Study of the effect of inorganic inhibitor on the calcium carbonate precipitation in the localized irrigation systems, Nanotechnol. Environ. Eng., 6 (2021) 1–8.
[20] M. Belattar, A. Hadfi, S. Ben-Aazza, S. Mohareb, I. Karmal, N. Hafid, A. Driouiche, Kinetic study of the scaling power of sanitary water in the tourist area of Agadir, Mater. Today:. Proc., 22 (2020) 61–63.
[21] S. Ben-aazza, A. Hadfi, M. El Housse, M. Belattar, S. Mohareb, I. Karmal, N. Hafid, A. Driouiche, Effect of commercial product "LEVALL®28" on the inhibition of scaling's water, Groundwater Sustainable Dev., 12 (2021) 100492, doi: 10.1016/j.gsd.2020.100492.
[22] M. Belattar, A. Hadfi, S. Ben-Aazza, I. Karmal, S. Mohareb, M. El Housse, N. Hafid, A. Driouiche, Efficiency of one scale inhibitor on calcium carbonate precipitation from hot water sanitary: effect of temperature and concentration, Heliyon, 7 (2021) e06152, doi: 10.1016/j.heliyon.2021.e06152.
[23] P. Zhang, P. Knötig, S. Gray, M. Duke, Scale reduction and cleaning techniques during direct contact membrane distillation of seawater reverse osmosis brine, Desalination, 374 (2015) 20–30.
[24] W.Y. Shih, A. Rahardianto, R.W. Lee, Y. Cohen, Morphometric characterization of calcium sulfate dihydrate (gypsum) scale on reverse osmosis membranes, J. Membr. Sci., 252 (2005) 253–263.
[25] W.-Y. Shih, K. Albrecht, J. Glater, Y. Cohen, A dual-probe approach for evaluation of gypsum crystallization in response to antiscalant treatment, Desalination, 169 (2004) 213–221.
[26] M. Aziz, G. Kasongo, Scaling prevention of thin film composite polyamide Reverse Osmosis membranes by Zn ions, Desalination, 464 (2019) 76–83.
[27] J.K. Fink, Chapter 7 – Scale Inhibitors, in: Petroleum Engineer's Guide to Oil Field Chemicals and Fluids, Gulf Professional Publishing, 2012, pp. 253–274.
[28] K. Chauhan, R. Kumar, M. Kumar, P. Sharma, G.S. Chauhan, Modified pectin-based polymers as green antiscalants for calcium sulfate scale inhibition, Desalination, 305 (2012) 31–37.
[29] F. Hui, J. Lédion, Evaluation methods for the scaling power of water, J. Eur. D Hydrol., 33 (2002) 55–74.
[30] C. Verma, E.E. Ebenso, I. Bahadur, M.A. Quraishi, An overview on plant extracts as environmental sustainable and green corrosion inhibitors for metals and alloys in aggressive corrosive media, J. Mol. Liq., 266 (2018) 577–590.
[31] Suharso, N.A. Sabriani, Tugiyono, Buhani, T. Endaryanto, Kemenyan (Styrax benzoin Dryand) extract as green inhibitor of calcium carbonate ($CaCO_3$) crystallization, Desal. Water Treat., 92 (2017) 38–45.
[32] B. Salehi, J. Sharifi-Rad, C. Quispe, H. Llaique, M. Villalobos, A. Smeriglio, D. Trombetta, S.M. Ezzat, M.A. Salem, A. Zayed, C.M. Salgado Castillo, S.E. Yazdi, S. Sen, K. Acharya, F. Sharopov, N. Martins, Insights into Eucalyptus genus chemical constituents, biological activities and health-promoting effects, Trends Food Sci. Technol., 91 (2019) 609–624.
[33] E. González-Burgos, M. Liaudanskas, J. Viškelis, V. Žvikas, V. Janulis, M.P. Gómez-Serranillos, Antioxidant activity, neuroprotective properties and bioactive constituents analysis of varying polarity extracts from *Eucalyptus globulus* leaves, J. Food Drug Anal., 26 (2018) 1293–1302.
[34] Y. Amakura, M. Yoshimura, N. Sugimoto, T. Yamazaki, T. Yoshida, Marker constituents of the natural antioxidant eucalyptus leaf extract for the evaluation of food additives, Biosci. Biotechnol. Biochem., 73 (2009) 1060–1065.
[35] S. Saleem, B. Ahmed, M.S. Khan, M. Al-Shaeri, J. Musarrat, Inhibition of growth and biofilm formation of clinical bacterial isolates by NiO nanoparticles synthesized from *Eucalyptus globulus* plants, Microb. Pathogen., 111 (2017) 375–387.
[36] H. Elfil, H. Roques, Role of hydrate phases of calcium carbonate on the scaling phenomenon, Desalination, 137 (2001) 177–186.

[37] H. Roques, A. Girou, Kinetics of the formation conditions of carbonate tartars, Water Res., 8 (1974) 907–920.
[38] Y. Boulahlib-Bendaoud, S. Ghizellaoui, M. Tlili, Inhibition of $CaCO_3$ scale formation in ground waters using mineral phosphates, Desal. Water Treat., 38 (2012) 382–388.
[39] I. Karmal, S. Mohareb, M. El housse, N. Hafid, A. Hadfi, M. Belattar, S. Ben-Aazza, A.A. Addi, R.A. Akbour, M. Hamdani, A. Driouiche, Structural and morphological characterization of scale deposits on the reverse osmosis membranes: case of brackish water demineralization station in Morocco, Groundwater Sustainable Dev., 11 (2020) 100483, doi: 10.1016/j.gsd.2020.100483.
[40] K. M. Kumar, B.K. Mandal, K. S. Kumar, P. S. Reddy, B. Sreedhar, Biobased green method to synthesise palladium and iron nanoparticles using Terminalia chebula aqueous extract, Spectrochim. Acta, Part A, 102 (2013) 128–133.
[41] M. Bagad, Z.A. Khan, Poly(n-butylcyanoacrylate) nanoparticles for oral delivery of quercetin: preparation, characterization, and pharmacokinetics and biodistribution studies in Wistar rats, Int. J. Nanomed., 10 (2015) 3921–3935.
[42] R.K. Das, B.B. Borthakur, U. Bora, Green synthesis of gold nanoparticles using ethanolic leaf extract of *Centella asiatica*, Mater. Lett., 64 (2010) 1445–1447.
[43] T. Wang, X. Jin, Z. Chen, M. Megharaj, R. Naidu, Green synthesis of Fe nanoparticles using eucalyptus leaf extracts for treatment of eutrophic wastewater, Sci. Total Environ., 466 (2014) 210–213.
[44] M.F.B. Sousa, F. Signorelli, C.A. Bertran, Fast evaluation of inhibitors for calcium carbonate scale based on pH continuous measurements in jar test at high salinity condition, J. Pet. Sci. Eng., 147 (2016) 468–473.
[45] K. Kezia, J. Lee, B. Zisu, M. Weeks, G. Chen, S. Gras, S. Kentish, Crystallisation of minerals from concentrated saline dairy effluent, Water Res., 101 (2016) 300–308.
[46] B. Coto, C. Martos, J.L. Peña, R. Rodríguez, G. Pastor, Effects in the solubility of $CaCO_3$: experimental study and model description, Fluid Phase Equilib., 324 (2012) 1–7.
[47] T. Waly, M.D. Kennedy, G.J. Witkamp, G. Amy, J.C. Schippers, On the induction time of $CaCO_3$: effect of ionic strength, Desal. Water Treat., 39 (2012) 55–69.
[48] M. Gritli, H. Cheap-Charpentier, O. Horner, H. Perrot, Y. B. Amor, Scale inhibition properties of metallic cations on $CaCO_3$ formation using fast controlled precipitation and a scaling quartz microbalance, Desal. Water Treat., 167 (2019) 113–121.
[49] M. Belattar, A. Hadfi, S. Ben-Aazza, S. Mohareb, I. Karmal, N. Hafid, A. Driouiche, Kinetic study of the scaling power of sanitary water in the tourist area of Agadir, Mater. Today:. Proc., 22 (2020) 61–63.
[50] S. Agarwal, R.K. Sairam, G.C. Srivastava, A. Tyagi, R.C. Meena, Role of ABA, salicylic acid, calcium and hydrogen peroxide on antioxidant enzymes induction in wheat seedlings, Plant Sci., 169 (2005) 559–570.